CORA Cork Open Research Archive
Cartlann Taighde Oscailte Chorcaí

Title	Frequency-dependent time-delays for strong outbursts in selected blazars from the Metsähovi and the University of Michigan Radio Astronomy Observatory monitoring databases – I
Authors	Pyatunina, T. B.;Kudryavtseva, N. A.;Gabuzda, Denise;Jorstad, S. G.;Aller, M. F.;Aller, H. D.;Teräsranta, H.
Publication date	2006
Original Citation	Pyatunina, T. B., Kudryavtseva, N. A., Gabuzda, D. C., Jorstad, S. G., Aller, M. F., Aller, H. D. and Teräsranta, H. (2006) 'Frequency-dependent time-delays for strong outbursts in selected blazars from the Metsähovi and the University of Michigan Radio Astronomy Observatory monitoring databases – I', Monthly Notices of the Royal Astronomical Society, 373(4), pp. 1470-1482. doi: 10.1111/j.1365-2966.2006.11068.x
Type of publication	Article (peer-reviewed)
Link to publisher's version	https://academic.oup.com/mnras/article-lookup/doi/10.1111/j.1365-2966.2006.11068.x - 10.1111/j.1365-2966.2006.11068.x
Rights	© 2006, the Authors. Journal compilation © 2006, RAS
Download date	2026-11-17 10:59:40
Item downloaded from	https://hdl.handle.net/10468/4982

UCC
University College Cork, Ireland
Coláiste na hOllscoile Corcaigh

Mon. Not. R. Astron. Soc. **373,** 1470–1482 (2006) doi:10.1111/j.1365-2966.2006.11068.x

Frequency-dependent time-delays for strong outbursts in selected blazars from the Metsähovi and the University of Michigan Radio Astronomy Observatory monitoring databases – I.

T. B. Pyatunina,[1⋆] N. A. Kudryavtseva,[2,3] D. C. Gabuzda,[4]† S. G. Jorstad,[5] M. F. Aller,[6] H. D. Aller[6] and H. Teräsranta[7]

[1]*Institute of Applied Astronomy, St. Petersburg, Russia*
[2]*Max-Plank-Institut für Radioastronomie, Auf dem Hügel 63, Bonn 53121, Germany*
[3]*St. Petersburg State University, Petrodvoretz, St. Petersburg, Russia*
[4]*Physics Department, University College Cork, Cork, Republic of Ireland*
[5]*Institute for Astrophysical Research, Boston University, Boston, MA 02215, USA*
[6]*Astronomy Department, Dennison Building, University of Michigan, MI 48109-1042, USA*
[7]*Metsähovi Radio Observatory, Helsinki University of Technology, Finland*

Accepted 2006 September 13. Received 2006 September 12; in original form 2006 January 12

ABSTRACT

The combined data of the University of Michigan Radio Astronomy Observatory and Metsähovi Radio Observatory provide us with radio light curves for active galactic nuclei monitored by both observatories from 4.8 to 37 GHz covering time-intervals up to ∼25 yr. We consider here such composite light curves for four gamma-ray blazars that have been nearly continuously monitored at both observatories: 0458−020, 0528+134, 1730−130 and 2230+114. We have decomposed the most prominent outbursts in the light curves of these four blazars into individual components using Gaussian model fitting, and estimated the epochs, amplitudes, and half-widths of these components as functions of frequency. We attempt to distinguish 'core outbursts', which show frequency-dependent time-delays and are associated with brightening of the core, from 'jet outbursts', which appear nearly synchronous at all frequencies and are accompanied by the emergence of new jet components and their subsequent evolution. The outbursts in 0528+134 and 2230+114 display fine structure and consist of individual suboutbursts. Available 43-GHz Very Long Baseline Array images allow us to identify only one pure core outburst (in 2230+114) and one pure jet outburst (0458−020). Most of the outbursts analysed are mixed, in the sense that they display frequency-dependent time-delays (i.e. they are optically thick) and are associated with the eventual emergence of new jet components. The maxima of the jet and mixed outbursts probably correspond to epochs when newly ejected components become fully optically thin. These epochs are also marked by a significant increase in the angular velocities of the ejected components. There is evidence that the outbursts in 2230+114 repeat every 8.0 ± 0.3 yr, with the positions of individual suboutbursts being preserved from one quasi-periodic eight-year cycle to another, even though their amplitudes vary by more than a factor of 2. Preliminary estimates of the total durations of possible activity cycles based on an analysis of total flux-density variations and all available very long baseline interferometry data are given for the remaining sources.

Key words: galaxies: active – quasars: individual: 0458−020 – quasars: individual: 0528+134 – quasars: individual: 1730−130 – quasars: individual: 2230+114.

1 INTRODUCTION

The term 'blazar' is sometimes used to refer to the subset of core-dominated active galactic nuclei (AGN) that display high-amplitude

⋆Deceased in 2005 August.
†E-mail: gabuzda@phys.ucc.ie

© 2006 The Authors. Journal compilation © 2006 RAS

variability over a wide range of wavebands, testifying that one of the relativistic jets in these objects is oriented close to the line of sight towards the Earth. The variability of blazars is a very complex phenomenon, and many different processes can take part, such as activity of the central engine, the propagation of primary perturbations down the jet, the evolution of the jet itself and various propagation effects (e.g. interaction with the surrounding medium) (Marscher 1996). During the last few years, important progress has been made in understanding many aspects of these phenomena through theoretical simulations (see Gómez 2005, and references therein), investigations of total flux variability in the X-ray (Pian 2003), gamma (Kranich 2003) and radio (Aller et al. 1999; Teräsranta, Wiren & Koivisto 2003) and various very long baseline interferometry (VLBI) studies (e.g. Britzen et al. 1999a; Gómez et al. 2000; Jorstad et al. 2005; Lister & Homan 2005).

Nevertheless, our understanding of the global, long-term development of the activity remains very fragmentary. The detection of periodicity in the activity of the blazars OJ287 ($P \sim 12$ yr, Pursimo et al. 2000), 0059+581 ($P \sim 4$ yr, Pyatunina et al. 2003), 0202+149 ($P \sim 4$ yr, Pyatunina et al. 2000) and 0235+164 ($P \sim 5.7$ yr, Raiteri et al. 2001) looks promising in this regard, but all attempts to estimate exact periods for the activity have been unconvincing, even for the best-sampled case of OJ287 (Kidger 2000), indicating that the phenomenon is probably not strictly periodic, but instead quasi-periodic. Indeed, even if the phenomena triggering a blazar's activity were purely periodic in nature, the observed variability would likely to be at best quasi-periodic, since it is the product of multiple complex processes associated with the generation and propagation of the radio emission. Numerical simulations of a binary black hole model for OJ287 (Sundelius et al. 1997) show that the triggering of the activity itself can be a complex function of time (see below), making the observed variability even more complex. Nevertheless, analysis of such quasi-periodicity can be an important diagnostic tool for modelling the energy generation in AGN and investigating binary black hole systems. Below we propose an alternative approach to investigate the global evolution of blazars.

Physically, the activity of a source can be described using two independent time-scales: $T_{\rm act}$, the characteristic time-scale for the activity of the central engine, and $T_{\rm ev}$, the time-scale for evolution of the jet after it has been disturbed by a perturbation at its base. The time-scale $T_{\rm ev}$ includes a whole sequence of events, from the initial appearance of the perturbation to the time when the propagating perturbation fades and merges into the quiescent jet emission. At present, it may be difficult to define this important time-scale observationally. The time-scale $T_{\rm act}$ can be thought of as the duration of one complete 'activity cycle', which we propose to define as the characteristic time-interval between two successive events marking onsets of phases of activity. With this definition, for example, a blazar that showed a pattern of being active for 5 yr, then quiescent for 10 yr, and then active for 5 yr, and so forth, would have $T_{\rm act} \simeq$ 15 yr. If the time-scale for activity exceeds the time-scale for the jet's evolution ($T_{\rm act} \geqslant T_{\rm ev}$), two subsequent activity cycles should be easily distinguishable; otherwise, manifestations of core activity and jet evolution associated with different cycles can be superimposed and complicate the observed picture. It should also be borne in mind that the observed $T_{\rm act}$ may be affected by the source's redshift, while the observed $T_{\rm ev}$ may be affected by both the redshift and the Doppler factor of the jet (for more detail, see the discussion in Lister 2001).

According to theoretical arguments (Marscher 1996; Gómez et al. 1997), a shock induced by a primary excitation at the base of the jet is initially manifest in radio light curves as an outburst that is delayed at lower frequencies due to the combined effects of the frequency stratification of the emitting electrons, non-zero opacity and light-travel delays. Such time-delayed outbursts are associated observationally on milliarcsecond (mas) scales with brightening of the VLBI core, and can be considered 'core' outbursts. The propagation of the shock downstream in the jet is revealed via the emergence of a new optically thin jet component (or components) in the VLBI image, sometimes accompanied by 'jet' outbursts, which evolve nearly synchronously at all frequencies in the radio light curve. The integrated monitoring data support the division of observed outbursts into such core and jet outbursts, at least in some sources (0202+149, Pyatunina et al. 2000; 0420−014, Zhou et al. 2000; 0059+581, Pyatunina et al. 2003). Thus, in practice, it is reasonable to approximate the duration of an activity cycle as the time-interval between two successive 'core' outbursts. The questions of how this interval varies from source to source and how stable it is for a particular source may be keys for our understanding of the activity's grand design.

The majority of blazars do not seem to display a well-defined activity cycle and associated time-scale $T_{\rm act}$, due in part to incompleteness of their monitoring data over sufficiently long time-scales (decades) and in part due to the complexity or nature of the underlying physical processes giving rise to the variability (see e.g. Lister 2001). In addition, the clarity with which an activity cycle in a given source is manifest may be very different at different frequencies, especially if they are fairly widely spaced. Combined analyses of multi-epoch VLBI observations and multifrequency light curves for those cases when a reasonably well-defined cycle can be identified across a range of frequencies show that the duration of the activity cycle can vary from source to source over a wide range: $T_{\rm act} \sim 4$ yr for 0059+581 ($z = 0.643$, Pyatunina et al. 2003), ∼12 yr for 0735+178 ($z = 0.424$, Carswell et al. 1974; Agudo et al. 2002) and ∼20 yr for 1308+326 ($z = 0.996$, Hewitt & Burbidge 1993; Pyatunina et al. 2004). As has been noted above, the question of the stability of the activity time-scale, or of the quasi-periodicity of the activity, in a particular source is more complex, not only because the relevant time-scales can be rather long, but also because of several other important factors. It has been suggested that a supermassive binary black hole in the nucleus of the AGN may be responsible for both the existence of quasi-periodicity (Lehto & Valtonen 1996; Valtaoja et al. 2000) and the activity itself (Sillanpää 1999), as well as for structural changes on parsec scales (Lobanov & Roland 2002). In this picture, activity can be triggered by the periodic tidal perturbation of the primary black hole's accretion disc by the orbital motion of a secondary black hole or the secondary's accretion disc. The eccentricity of the orbit (Lehto & Valtonen 1996; Sundelius et al. 1997) may divide the overall period in two unequal parts, while precession of the jet may change the viewing angle, resulting in modulation of the amplitudes of outbursts. Relativistic precession of the secondary's orbit will complicate the observed variability even more.

In our approach, we carry out a joint analysis of the total-flux and spectral variability based on multifrequency light curves, combined with the observed structural changes in VLBI images. This paper presents our results for a first small sample of four selected sources. The frequency-dependent time-delays found here can also be used to test models of the non-thermal emission in blazars (Gómez et al. 1997; Lobanov 1998; Marscher 2001).

2 DESCRIPTION OF THE DATA USED

The combined data from the University of Michigan Radio Astronomy Observatory (UMRAO; Aller et al. 1985) and Metsähovi

Radio Observatory (Teräsranta et al. 1998, 2004, 2005) provide us with radio light curves for ∼100 AGN from 4.8 to 37 GHz covering time-intervals up to ∼25 yr. A preliminary inspection of all available light curves shows that only about one-third display well-separated, bright outbursts with definite frequency-dependent time-delays that are suitable for analysis. As a first sample, we chose the four gamma-ray blazars 0458−020, 0528+134, 1730−130 and 2230+114, for which multi-epoch VLBI data are also available (Jorstad et al. 2001). The multifrequency light curves for these sources are shown in Figs 2, 4, 7 and 9. In all figures except for Fig. 7 (right-hand panel) and 12, the filled symbols correspond to integrated measurements and the hollow symbols to VLBI measurements; integrated measurements at 4.8 GHz are shown by the diamonds, at 8 GHz by the triangles, at 14.5 GHz by the circles, at 22 GHz by the squares, at 37 GHz by the stars and at 90 GHz by the pluses.

We separated the most-prominent outbursts in the radio light curves into individual components using Gaussian model fitting. We chose to fit Gaussian components for the simple reason that most of the observed centimetre-wavelength outbursts are symmetrical and have shapes that are approximately Gaussian; in particular, the shapes of the centimetre-wavelength outbursts do not correspond well to the exponential profiles used, for example, by Valtaoja et al. (1999) to fit millimetre flares. The highest of the five frequencies for which we obtained light curve decompositions is 37 GHz, while the exponential behaviour pointed out by Valtaoja et al. (1999) is manifest in frequencies of 90 and 230 GHz. Long-term trends in the total flux-density variations described using polynomial approximations for the deepest minima in the light curves were subtracted before the fitting. An example result of the long-term trend determination and Gaussian decomposition is shown in Fig. 1. This example illustrates the general criterion that the smallest number of Gaussians providing a complete description of the light curve was used. The number of Gaussians used depended on the time-interval covered by the light curve and the characteristic time-scale for the source variability.

The light curves of the sources considered here could all be decomposed into Gaussian components with goodness of fit satifying the χ^2 test at a significance level of 0.01. The frequency-dependent time-delays for individual components, $\Delta T_{\max}(\nu) = T_{\max}(\nu) - T_{\max}(\nu_0)$, where ν_0 is the highest frequency observed, were determined and approximated by exponential functions of frequency of the form $\Delta T_{\max}(\nu) \propto \nu^{\alpha}$ (Gómez et al. 1997; Lobanov 1998). The results of these approximations are summarized in Table 6.

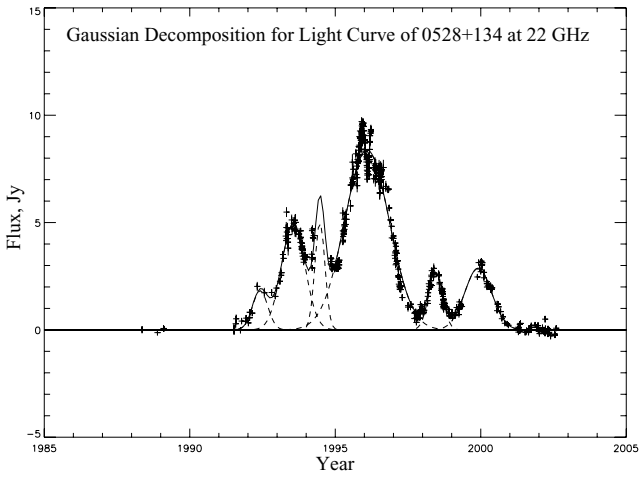


Figure 1. Example of our Gaussian decompositions of the light curves: light curve for 0528+134 at 22 GHz.

The individual parameters of the outbursts as derived from the Gaussian model fitting are given in Tables 1–3 and 5, whose columns present (1) the component notation, (2) the observing frequency, (3) the epoch of the maximum flux, (4) the maximum amplitude, (5) the full width at half-maximum of the Gaussian describing the outburst, and (6) the time-delay for the given frequency; when the formal errors on the epoch of maximum, Gaussian width and time-delay were occasionally smaller than 0.01 yr, we set these errors equal to 0.01 yr. Essentially all the Gaussian component fits are included in these tables; the exception is that the Gaussian fits for the light curve of 1730−130 prior to $\simeq$ 1993 were not included, since they all displayed very small frequency delays and small amplitudes compared to the powerful outburst of 1996.

3 0458−020, $Z = 2.27$

The radio light curve of this distant quasar displays three distinct outbursts with declining amplitudes at epochs 1989.1, 1992.8 and 1995.4 in the period 1984–2002, which we label A, B and C, respectively (Fig. 2, left-hand panel). A comparison of the 37-GHz light curve and the combined 90-GHz light curve based on the data of Steppe et al. (1988, 1992, 1993) and Reuter et al. (1997) indicates that at least outburst A (1989.06) may have some fine structure that is unresolved in the available data (Fig. 2, right-hand panel). The individual parameters of the outbursts as derived from the Gaussian model fitting are given in Table 1, and the time-delays for these outbursts as functions of frequency are shown in Fig. 3. Only outburst A displays frequency-dependent time-delays, and may be associated with a strong primary perturbation in the core. Outbursts B (1992.81) and C (1995.40) show no time-delays, and can accordingly be considered jet outbursts. The evolution of the source's structure at 43 GHz (Jorstad et al. 2001) shows the appearance of the new jet component B2 during 1995–1998. The variations of the 43-GHz flux densities of the core and B2 shown in Fig. 2 (right-hand panel) are consistent with the classification of outburst C as a jet outburst.

Unfortunately, we have no high-resolution VLBI images for the period prior to 1995, and our classification of outbursts A (a core outburst) and B (a jet outburst) cannot be confirmed by direct investigation of the structural evolution. The only candidate for a jet component that could be associated with outburst B is the component B1 detected in 43-GHz maps at epochs 1995.31 and 1995.47. The radial distance of this component from the core is about 0.8 mas. If the rates of angular separation from the core for components B1 and B2 are similar, the zero-separation time for component B1 is near 1990. Therefore, there is some possibility that the emergence and evolution of this component can be linked to outburst B.

We cannot identify the overall duration of the activity cycle in this source, $T_{\rm act}$, because the available monitoring data spanning 16 yr include only one core outburst, and it is precisely the time-interval between core outbursts that determines $T_{\rm act}$. The only thing we can do at this stage is to give a lower limit for the total duration of each activity cycle, $T_{\rm act} \geqslant 16$ yr, and to suggest that it appears that the activity cycles in 0458−020 include a core outburst (as in 1989.06) followed by at least two jet outbursts (as in 1992.81 and 1995.41).

It is interesting that a comparison of the 15-GHz maps from the MOJAVE database (Lister & Homan 2005) for epochs 2001 March 15 and 2003 March 1 shows an increase in the peak flux between these two epochs, from 0.76 to 1.045 Jy. This brightening of the core could be an indication of the beginning of a new activity cycle in

Table 1. 0458−020. Parameters of outbursts.

Component	Frequency (GHz)	$T_{\max}$ (yr)	Amplitude (Jy)	Θ (yr)	Time-delay (yr)
A	37	1989.06 ± 0.02	2.589 ± 0.038	2.65 ± 0.07	0
	22	1989.16 ± 0.02	3.292 ± 0.074	2.82 ± 0.08	0.09 ± 0.03
	14.5	1989.40 ± 0.02	3.066 ± 0.013	3.65 ± 0.03	0.34 ± 0.03
	8	1989.79 ± 0.02	2.465 ± 0.010	2.83 ± 0.02	0.73 ± 0.03
	4.8	1989.99 ± 0.01	2.490 ± 0.007	3.02 ± 0.01	0.93 ± 0.03
B	37	1992.81 ± 0.04	1.700 ± 0.034	3.23 ± 0.15	0
	22	1992.76 ± 0.03	2.378 ± 0.053	2.95 ± 0.16	-0.05 ± 0.05
	14.5	1993.09 ± 0.01	2.225 ± 0.018	1.54 ± 0.02	0.28 ± 0.05
	8	1992.99 ± 0.01	1.841 ± 0.012	1.73 ± 0.02	0.18 ± 0.05
	4.8	1993.09 ± 0.01	1.780 ± 0.013	1.57 ± 0.01	0.28 ± 0.04
C	37	1995.41 ± 0.02	1.295 ± 0.054	1.11 ± 0.06	0
	22	1995.37 ± 0.04	1.272 ± 0.028	1.66 ± 0.05	-0.04 ± 0.04
	14.5	1995.17 ± 0.02	1.639 ± 0.012	1.94 ± 0.02	-0.24 ± 0.02
	8	1995.34 ± 0.03	1.134 ± 0.013	2.38 ± 0.04	-0.07 ± 0.04

Table 2. 0528+134. Parameters of outbursts.

Component	Frequency (GHz)	$T_{\max}$ (yr)	Amplitude (Jy)	Θ (yr)	Time-delay (yr)
A	90	1992.15 ± 0.02	5.10 ± 0.26	0.80 ± 0.02	-0.06 ± 0.02
	37	1992.21 ± 0.01	2.415 ± 0.042	0.93 ± 0.02	0
	22	1992.42 ± 0.01	1.83 ± 0.17	0.62 ± 0.04	0.21 ± 0.02
	14.5	1992.51 ± 0.01	1.124 ± 0.043	0.63 ± 0.06	0.30 ± 0.02
B	90	1993.51 ± 0.01	5.12 ± 0.11	0.90 ± 0.01	0.03 ± 0.02
	37	1993.48 ± 0.01	5.310 ± 0.050	0.97 ± 0.01	0
	22	1993.56 ± 0.01	4.927 ± 0.062	0.96 ± 0.02	0.08 ± 0.01
	14.5	1993.65 ± 0.01	2.634 ± 0.025	1.25 ± 0.04	0.18 ± 0.01
	8	1993.62 ± 0.02	1.564 ± 0.021	1.55 ± 0.07	0.14 ± 0.02
	4.8	1993.64 ± 0.02	0.736 ± 0.012	0.80 ± 0.02	0.16 ± 0.02
C	90	1994.45 ± 0.02	4.03 ± 0.68	0.40 ± 0.03	0.01 ± 0.18
	37	1994.44 ± 0.01	4.13 ± 0.25	0.48 ± 0.01	0
	22	1994.47 ± 0.01	5.01 ± 0.19	0.41 ± 0.01	0.03 ± 0.01
	14.5	1994.52 ± 0.01	2.311 ± 0.031	0.64 ± 0.01	0.08 ± 0.01
	8	1994.52 ± 0.01	1.921 ± 0.040	0.59 ± 0.01	0.07 ± 0.01
	4.8	1994.55 ± 0.01	1.329 ± 0.023	0.69 ± 0.01	0.11 ± 0.01
D	37	1995.92 ± 0.01	7.490 ± 0.032	1.76 ± 0.01	0
	22	1996.09 ± 0.01	8.385 ± 0.023	1.81 ± 0.01	0.16 ± 0.01
	14.5	1996.19 ± 0.01	7.327 ± 0.021	1.56 ± 0.01	0.27 ± 0.01
	8	1996.33 ± 0.01	6.725 ± 0.017	1.90 ± 0.01	0.41 ± 0.01
	4.8	1996.58 ± 0.01	3.694 ± 0.013	1.97 ± 0.01	0.65 ± 0.01
E	37	1998.37 ± 0.01	2.338 ± 0.073	0.62 ± 0.01	0
	22	1998.44 ± 0.01	2.626 ± 0.040	0.57 ± 0.01	0.07 ± 0.01
	14.5	1998.49 ± 0.01	1.661 ± 0.025	0.44 ± 0.01	0.12 ± 0.01
	8	1998.67 ± 0.01	1.441 ± 0.020	0.77 ± 0.01	0.30 ± 0.01
	4.8	1998.81 ± 0.02	0.844 ± 0.024	0.96 ± 0.04	0.44 ± 0.02
F	37	1999.82 ± 0.01	2.801 ± 0.076	1.03 ± 0.02	0
	22	1999.91 ± 0.01	2.874 ± 0.031	1.09 ± 0.01	0.09 ± 0.02
	14.5	2000.16 ± 0.01	1.788 ± 0.012	0.93 ± 0.01	0.34 ± 0.02
	8	2000.29 ± 0.02	1.474 ± 0.012	1.36 ± 0.02	0.47 ± 0.02
	4.8	2000.67 ± 0.04	0.905 ± 0.011	2.04 ± 0.04	0.85 ± 0.04

this source. Support for the onset of a new activity cycle can also be found in the 43-GHz maps from the Radio Reference Frame Image Database (RRFID; http://rorf/usno.navy.mil/rrfid.shtml). The peak flux density in the 43-GHz map for 2003 September 13 exceeds the peak flux density in the map for 2002 December 26 by more than a factor of 2 ($S_{\rm peak} = 1.42$ Jy beam^{-1} as opposed to 0.607 Jy beam^{-1}).

If our lower limit for the characteristic durations of activity cycles in 0458−020 is correct, the maximum of the previous cycle should have been sometime before 1973. Early monitoring data at 7.9 GHz (Dent & Kapitzky 1976) covering the time-interval 1971–1974.5 display a moderate outburst with its maximum flux, $S = 2.86 \pm 0.09$ Jy, occurring near 1973. Some indications of activity during

Table 3. 1730−130. Parameters of outbursts.

Component	Frequency (GHz)	T_{max} (yr)	Amplitude (Jy)	Θ (yr)	Time-delay (yr)
A	37	1996.26 ± 0.01	12.22 ± 0.22	2.00 ± 0.03	0
	22	1996.30 ± 0.02	11.28 ± 0.17	2.11 ± 0.03	0.04 ± 0.02
	14.5	1996.37 ± 0.01	10.139 ± 0.031	2.09 ± 0.01	0.11 ± 0.01
	8	1996.78 ± 0.01	7.091 ± 0.020	2.03 ± 0.01	0.53 ± 0.01
	4.8	1997.19 ± 0.01	3.379 ± 0.017	2.02 ± 0.02	0.93 ± 0.02

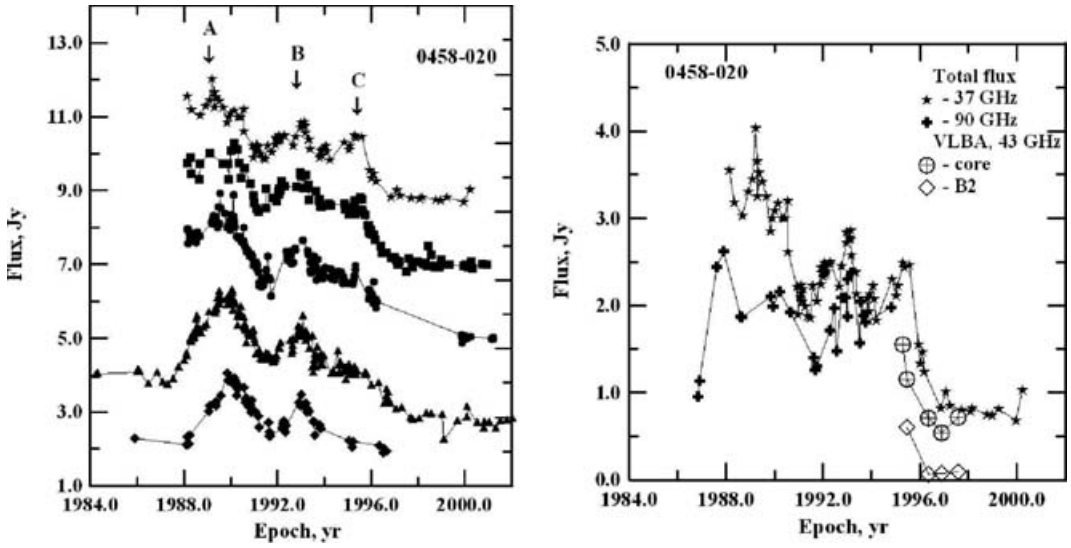


Figure 2. 0458−020. Left-hand side: from top to bottom panel, light curves for 37, 22, 14.5, 8 and 4.8 GHz. The light curves have been shifted upwards by 8, 6, 4, 1.5 and 0 Jy, respectively. Right-hand panel: light curves at 37 (filled stars) and 90 GHz (filled pluses) combined with the flux-density variations of two components in the 43-GHz maps of Jorstad et al. (2001).

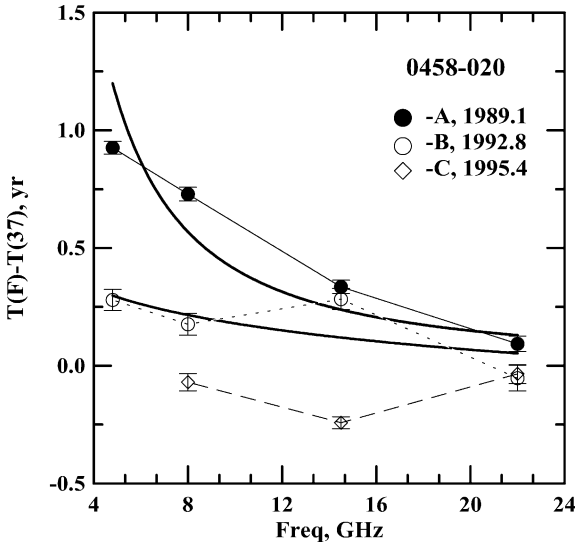


Figure 3. 0458−020. Time-delays as functions of frequency. The bold curves show exponential fits to the observed time-delays.

the interval 1968–1979 can be found in the 5-GHz monitoring data of Wright (1984) as well. These data show that 0458−020 was variable during this period, with a mean flux of $S_{mean} = 1.76$ Jy and an rms dispersion of 14 per cent. For comparison, the dispersion for the quasar 3C 454.3, which displays a strong outburst during this period (UMRAO data), was estimated to be 34 per cent. Thus, it seems probable that 0458−020 was active during this period, although the level of activity was probably not as strong as during the activity cycle observed in roughly 1986–2002.

4 0528+134, $Z = 2.06$

The radio light curve of this quasar did not display bright events until 1990, when a strong and complex outburst started. The outburst displays at least six narrow components (Fig. 4, left-hand panel), whose parameters based on the Gaussian model fitting are given in Table 4. The 37-GHz light curve shows the possible existence of additional fine structure in outburst D that is unresolved by the Gaussian model fitting. As was shown by Zhang et al. (1994), the spectrum of 0528+134 changed dramatically at the end of the 1980s, when its turnover frequency moved from near 8 GHz to near 100 GHz. A comparison of the 37-GHz (Metsähovi) and 90-GHz light curves (see references above and Krichbaum et al. 1997) shows the spectral evolution during this period. The amplitudes of individual outbursts as functions of frequency in Fig. 5 show a shift of the turnover frequency in time, from above 90 GHz (A) to ∼14.5 GHz (D). In addition, there is a sudden decrease in the amplitudes of outbursts E and F compared to the earlier outbursts. The quasar 0528+134 is one of the brightest gamma-ray sources. The dates

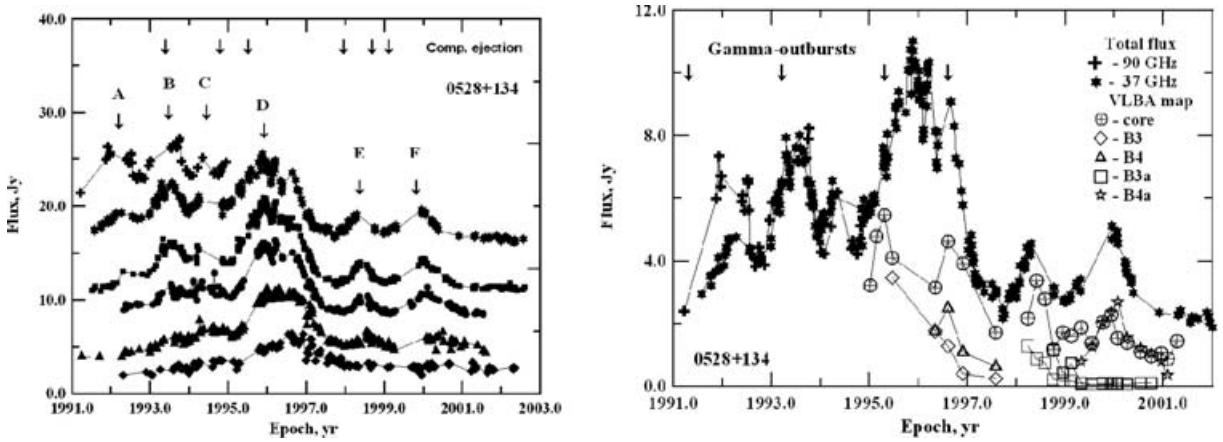


Figure 4. 0528+134. Left-hand side: from top to bottom panel, light curves for 37, 22, 14.5, 8 and 4.8 GHz. The light curves have been shifted upwards by 14.5, 9, 6, 2 and 0 Jy, respectively. Right-hand panel: light curves at 37 and 90 GHz combined with the flux-density variations of individual components in the 43-GHz maps of Jorstad et al. (2001, 2005). The positions of bright gamma-ray flares are shown by the arrows.

Table 4. 2230+114. Quasi-period in activity.

Frequency	Cycle 1		Cycle 2		Cycle 3		P(2-1)	P(3-2)
	Component	T_{max}	Component	T_{max}	Component	T_{max}		
37			A2	1989.57	A3	1997.48		7.91
22			A2	1989.67	A3	1997.90		8.22
14.5	A1	1981.36	A2	1989.74	A3	1998.00	8.39	8.25
8	A1	1981.40	A2	1989.95	A3	1998.34	8.55	8.39
37			B2	1990.50	B3	1997.92		7.42
22			B2	1990.54	B3	1998.57		8.02
14.5	B1	1982.71	B2	1990.63	B3	1998.62	7.92	7.98
8	B1	1982.94	B2	1990.84	B3	1999.09	7.89	8.25
37			C2	1991.38	E3	1998.86		7.48
22			C2	1991.38	C3	1999.02		7.64
37			D2	1992.10	D3	2000.01		7.91
22			D2	1992.09	D3	1999.84		7.76
14.5	C1+D1	1983.68	C2+D2	1991.98	C3+D3	1999.75	8.3	7.76
8	C1+D1	1983.97	C2+D2	1991.71	C3+D3	2000.03	7.74	8.32
4.8	C1+D1	1984.08	C2+D2	1992.25			8.17	

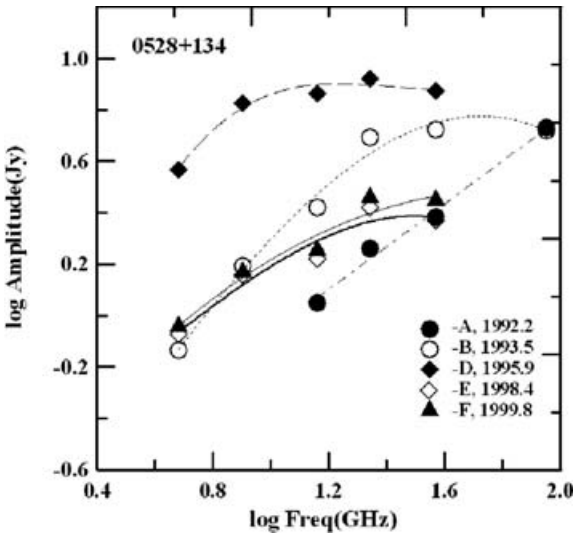


Figure 5. 0528+134. Suboutburst amplitudes as functions of frequency. The curves show exponential fits to the observed amplitudes for suboutbursts A (dot–dashed line), B (dotted line), D (dashed line) and E/F (solid line).

of four EGRET flares with fluxes $>12 \times 10^{-7}$ photon cm^{-2} s^{-1} detected during 1991–1997 (Mukherjee et al. 1999) are shown by the arrows in Fig. 4 (right-hand panel). The brightest flare (1993 March 23–29; $T \sim 1993.2$) coincides with outburst B, while the brightest radio outburst (D) seems to be associated with a moderate, prolonged gamma-ray flare observed from 1995 April 4 to June 6 and a moderate flare detected in 1996 August 20–27. It is interesting that the brightest gamma-ray flare coincides with the brightest 90-GHz outburst, B, but precedes the maximum of the brightest outburst at 37 GHz. The spectral evolution combined with the gamma-ray emission suggests that probably not all the peaks observed in the 0528+134 light curves represent individual outbursts, but are instead made of a series of finer suboutbursts that combine to form what appears to be a single complex observed outburst. The parameters of the Gaussian component fits at 90 GHz are very uncertain due to the relatively poor sampling, and we adopt 37 GHz as a reference frequency for determining the time-delays. The delay between 90 and 37 GHz averaged over suboutbursts A, B and C is -0.006 ± 0.045. The frequency-dependent time-delays for the suboutbursts are shown in Fig. 6. The time-delays for the first suboutburst, A ($\sim$1992.1), are determined only at $\nu \geqslant 14.5$ GHz, since these flares did not appear at the longer wavelengths. The time-delays at cm

© 2006 The Authors. Journal compilation © 2006 RAS, MNRAS **373,** 1470–1482

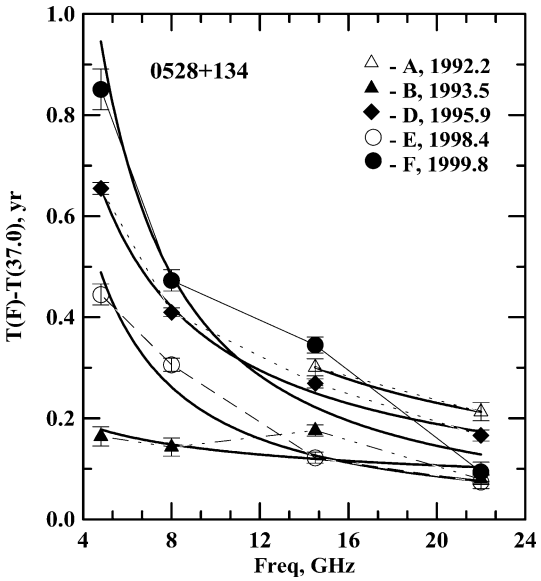


Figure 6. 0528+134. Time-delays as functions of frequency. The bold curves show exponential fits to the observed time-delays.

wavelengths are very small, even for suboutburst B (Fig. 6). Unfortunately, suboutburst C (∼1994.4) coincides with a gap in the Metsähovi data, and the time-delays given in Table 4 should be considered tentative. The time-delays of the later suboutbursts D, E and F vary over approximately a factor of 2, from 0.444 to 0.850 yr.

High-frequency (22–86 GHz) VLBI monitoring during 1992–1997 (Zhang et al. 1994; Krichbaum et al. 1995, 1997; Pohl et al. 1995) has revealed the appearance of five new jet components, which appear to be associated with suboutbursts A (component N1, Krichbaum et al. 1995), B (component N2, Krichbaum et al. 1995), C (component N3, Krichbaum et al. 1997) and D (components N4 and N5, Krichbaum et al. 1997). The multi-epoch imaging at 43 GHz of Jorstad et al. (2001, 2005) confirms the emergence of jet components associated with suboutbursts B (component B2), C (component B3) and D (component B4), and has also revealed two new jet components (B3a and B4a) associated with suboutbursts E and F. Thus, in contrast to the situation with the outbursts in 0458−020, suboutbursts A, B, C, D, E and F all show signatures of both 'core' outbursts (frequency-dependent time-delays) and 'jet' outbursts (association with the appearance of new superluminal components). The time variations of the flux densities of the core and individual jet components according to the data (Jorstad et al. 2001, 2005) are shown in Fig. 4 (right-hand panel).

As we noted above, this outburst is the brightest event in this object since 1976. However, low-amplitude flux-density variations were also observed at cm wavelengths during the period of low activity (1977–1991). Analysis of 8-GHz geodetic VLBI observations over nearly eight years from 1986.25 to 1994.07 made by Britzen et al. (1999b) has revealed, apart from the component N2 mentioned above (Krichbaum et al. 1997, component **a** in the notation of Britzen et al.), several superluminal jet components ejected prior to 1990. It is interesting that the position angles (PAs) of the previously ejected components **c** ($T_0 = 1984.4 \pm 2.3$, PA $\sim 180^\circ$) and **d** ($T_0 = 1982.1 \pm 2.3$, PA $\sim 150^\circ$) differ significantly from the position angle of component **a** ($T_0 = 1992.1 \pm 0.4$, PA ~ 70) (Britzen et al. 1999b). Thus, it seems that we can identify different light curves for 0528+134 for two different periods characterized by low (1977–1991) and high (1991–2004) activity. The difference between the observed levels of activity during these two periods could be due to variations of the jet's orientation (Zhang et al. 1994) or some other reasons internal to the source. It is interesting that the fine structure of the 8-GHz outburst seems to be less prominent during the low-activity period. The low level of activity and absence of high-frequency monitoring data hinder the detection and comparison of fine structure of the outbursts observed in the period of high and low activity. We estimate the characteristic duration of one activity cycle in the source to be $\geqslant 14$ yr. Component **b** (Britzen et al. 1999b), which was ejected during the period of low activity ($T_0 = 1988.4 \pm 1.0$) in PA $\sim 50^\circ$, does not fit into the picture we have outlined. Further high-frequency single-dish and/or VLBI observations are necessary to test our proposed picture.

5 1730−130 (NRAO 530), $Z = 0.90$

This quasar has displayed a single bright outburst in ∼35 yr of cm wavelength monitoring from 1967 to 2003 (Fig. 7, left-hand panel), first detected as an extremely narrow and bright flare at 230 GHz (Bower et al. 1997). The combined 90- and 230-GHz monitoring data (Steppe et al. 1993; Reuter et al. 1997) reveal two fainter outbursts near 1993 and 1994.5, which probably precede the 230-GHz flare (Fig. 7, right-hand panel) detected by Bower et al. (1997). All the outbursts coincide with epochs when gamma-ray flares with fluxes $>7 \times 10^{-7}$ photon cm^{-2} s^{-1} were detected, marked in the figure by the arrows (Mukherjee et al. 1997). The brightest gamma-ray flare (∼1995.45) occurs slightly after the main 230-GHz outburst, but precedes the main maximum at mm wavelengths. A comparison of the 90- and 37-GHz light curves reveals some traces of fine structure, at least at high frequencies. The parameters of the outburst are given in Table 5, and the time-delays as functions of frequency are shown in Fig. 8.

86-GHz VLBI maps obtained at epochs ∼1993.3 (Lobanov, Krichbaum & Graham 2000) and 1995.35 (Bower et al. 1997) show the core and two jet components that could have been ejected during the 1993 and 1994.5 outbursts, but we do not have enough information to be sure about this. A 43-GHz Very Long Baseline Array (VLBA) imaging (Jorstad et al. 2001) shows faint traces of a component that was probably ejected prior to 1995 (B1, $T_0 = 1994.57 \pm 0.17$) and a new component that was apparently ejected during the bright outburst (B2, $T_0 = 1995.54 \pm 0.05$). The variations of the flux densities of the core and the new component B2 are shown in Fig. 7 (right-hand panel). Thus, the outburst exhibits signs of both core and jet outbursts, like the outbursts observed in 0528+134.

If we consider the 1993 and 1994.5 outbursts to be precursors of the main outburst in 1996, the total duration of the activity cycle of the source may correspond to the time-interval from 1992 until 2001, when the 22- and 37-GHz fluxes began to grow again: $T_{\rm act} \simeq 9$ yr. In this case, the previous core outburst would have peaked in 1987, and the UMRAO monitoring data (Fig. 7, left-hand panel) do show a modest outburst at that epoch that seems to peak earliest at 14.5 GHz and latest at 4.8 GHz (i.e. consistent with a core outburst). Some further support for this estimate for $T_{\rm act}$ is provided in the MOJAVE (15 GHz, Lister & Homan 2005) and RRFID (24 and 43 GHz, Fey et al. 2005) databases. The 15-GHz VLBI maps show that both the total and the peak flux densities grew by more than a factor of 2 between 2000 January 11 and 2002 October 9, testifying to the onset of a new outburst. The 15-GHz peak flux densities for 2002 October 9, 2004 February 11, 2005 March 23 and 2005 July 24 are 4.74, 3.33, 2.83 and 2.30 Jy beam^{-1}, respectively. This sequence can be supplemented with the peak flux densities in the 24-GHz VLBI images reduced to the beam size for the 2003

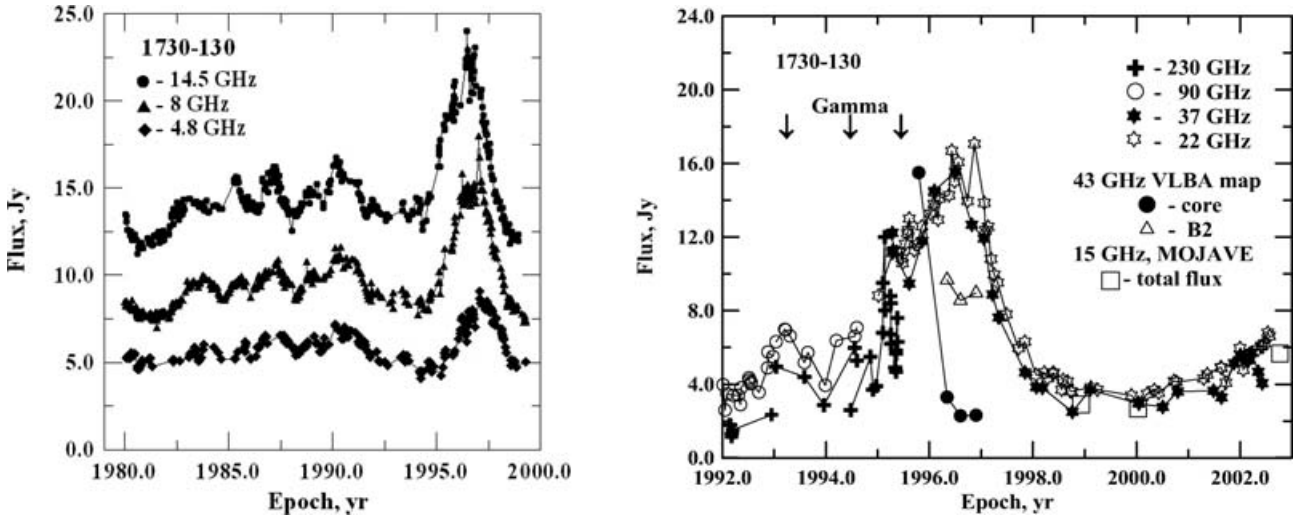


Figure 7. 1730−130. Left-hand side: from top to bottom panel, light curves for 14.5, 8 and 4.8 GHz shifted upwards by 8, 3 and 0 Jy, respectively. Right-hand panel: light curves at 22 and 37 GHz (both Metsähovi), and 90 and 230 GHz (Steppe et al. 1993; Bower et al. 1997; Reuter et al. 1997) combined with the flux-density variations of two individual components in the 43-GHz maps of Jorstad et al. (2001, 2005) and the total VLBI flux densities measured in the three MOJAVE images. The positions of gamma-ray flares are marked by the arrows.

Table 5. 2230+114. Parameters of outbursts.

Component	Frequency (GHz)	T_{max} (yr)	Amplitude (Jy)	Θ (yr)	Time-delay (yr)
A2	37	1989.57 ± 0.01	1.649 ± 0.050	0.74 ± 0.03	0
	22	1989.67 ± 0.02	1.21 ± 0.11	0.68 ± 0.08	0.10 ± 0.02
	14.5	1989.74 ± 0.01	1.328 ± 0.026	0.70 ± 0.03	0.17 ± 0.01
	8	1989.95 ± 0.02	0.730 ± 0.024	0.80 ± 0.04	0.38 ± 0.02
	4.8	1989.94 ± 0.02	0.318 ± 0.040	0.40 ± 0.19	0.37 ± 0.02
A3	37	1997.48 ± 0.01	3.656 ± 0.058	0.57 ± 0.08	0
	22	1997.90 ± 0.01	3.831 ± 0.030	0.83 ± 0.03	0.42 ± 0.01
	14.5	1998.00 ± 0.01	2.284 ± 0.024	0.90 ± 0.02	0.52 ± 0.01
	8	1998.34 ± 0.01	1.411 ± 0.023	0.67 ± 0.05	0.86 ± 0.01
B2	37	1990.50 ± 0.01	1.736 ± 0.050	0.55 ± 0.02	0
	22	1990.54 ± 0.01	1.59 ± 0.10	0.62 ± 0.05	0.04 ± 0.01
	14.5	1990.63 ± 0.01	1.418 ± 0.027	0.66 ± 0.02	0.13 ± 0.01
	8	1990.84 ± 0.01	0.965 ± 0.021	0.71 ± 0.03	0.33 ± 0.01
	4.8	1990.92 ± 0.03	0.702 ± 0.014	1.34 ± 0.08	0.42 ± 0.03
B3	37	1997.92 ± 0.01	3.630 ± 0.059	0.55 ± 0.03	0
	22	1998.57 ± 0.01	2.83 ± 0.11	0.48 ± 0.06	0.64 ± 0.01
	14.5	1998.62 ± 0.01	2.109 ± 0.018	0.66 ± 0.02	0.69 ± 0.01
	8	1999.09 ± 0.01	1.766 ± 0.026	0.69 ± 0.02	1.16 ± 0.01

May 23 15-GHz observations: 3.7, 3.8 and 2.9 Jy beam^{-1} for 2002 May 16, 2002 August 26 and 2003 May 23, respectively. Overall, these data clearly indicate a strong outburst in the VLBI core that seems to have peaked in $\simeq$2002–2003. The decrease in the peak flux densities at later epochs does not seem to be accompanied by the appearance of any new structure, although there are clear changes in the polarization of the core region between the first two 15-GHz epochs, overall suggesting that the 2002–2003 outburst may have been confined to the core. It is possible that the 1996 outburst and 2002–2003 outburst are associated with successive activity cycles in the source; if the 2002–2003 outburst is a 'precursor' to a main core outburst occurring in 2005, this could be consistent with our estimated cycle duration $T_{act} \simeq 9$ yr (recall that the 'precursor' outbursts for the major 1996 outburst occurred in 1993–1994), but further information about the spectrum of the 2002–2003 outburst and further VLBI monitoring are needed to test this hypothesis.

6 2230+114 (CTA 102), $Z = 1.04$

Radio light curves of this quasar display strong outbursts that repeat approximately every ∼8 yr (Fig. 9). At mm wavelengths, the outbursts can be decomposed into the six narrow suboutbursts A, B, C, D, E and F (Fig. 9, below right-hand panel); only the two leading suboutbursts A and B can be distinguished at cm wavelengths, while the other suboutbursts merge into two broad features (C+D and E+F; Fig. 9, below left-hand panel).

To test whether there is quasi-periodicity in the appearance of the outbursts, we subtracted the epochs for corresponding suboutbursts

© 2006 The Authors. Journal compilation © 2006 RAS, MNRAS **373,** 1470–1482

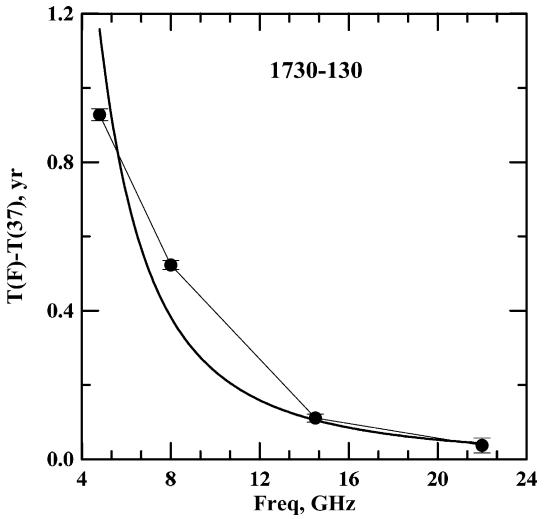


Figure 8. 1730−130. Time-delays as functions of frequency. The bold curves show exponential fits to the observed time-delays.

in consecutive cycles at all available wavelengths (Table 6). The mean time-intervals between the peaks of consecutive corresponding suboutbursts are 8.14 ± 0.30 for the interval from cycle 2 to cycle 1 and 7.95 ± 0.31 for the interval from cycle 3 to cycle 2. Given the time-delays between the various frequencies and the possible dependence of these time-delays on the amplitudes of individual suboutbursts (see below), the agreement between these two mean values is good. Therefore, we tentatively suggest that outbursts in this source repeat every 8.04 ± 0.30 yr, preserving the relative positions in time of individual suboutbursts within the outbursts, even when the amplitudes of the suboutbursts change substantially.

In this case, we expect that the leading suboutburst of the next outburst reached its maximum at 37 GHz near 2005.5 ± 0.3, and its maximum at $\simeq 15$ GHz near 2006.0 ± 0.3. The MOJAVE VLBI images clearly indicate an outburst in the VLBI core starting sometime in the second half of 2004: the observed peak flux densities for successive epochs are 1.05 (2004 April 10), 1.87 (2005 February 5), 2.00 (2005 September 19), 3.94 (2005 December 22) and 4.40 Jy beam^{-1} (2006 February 12). This may well represent the predicted leading suboutburst of the next outburst cycle, but further

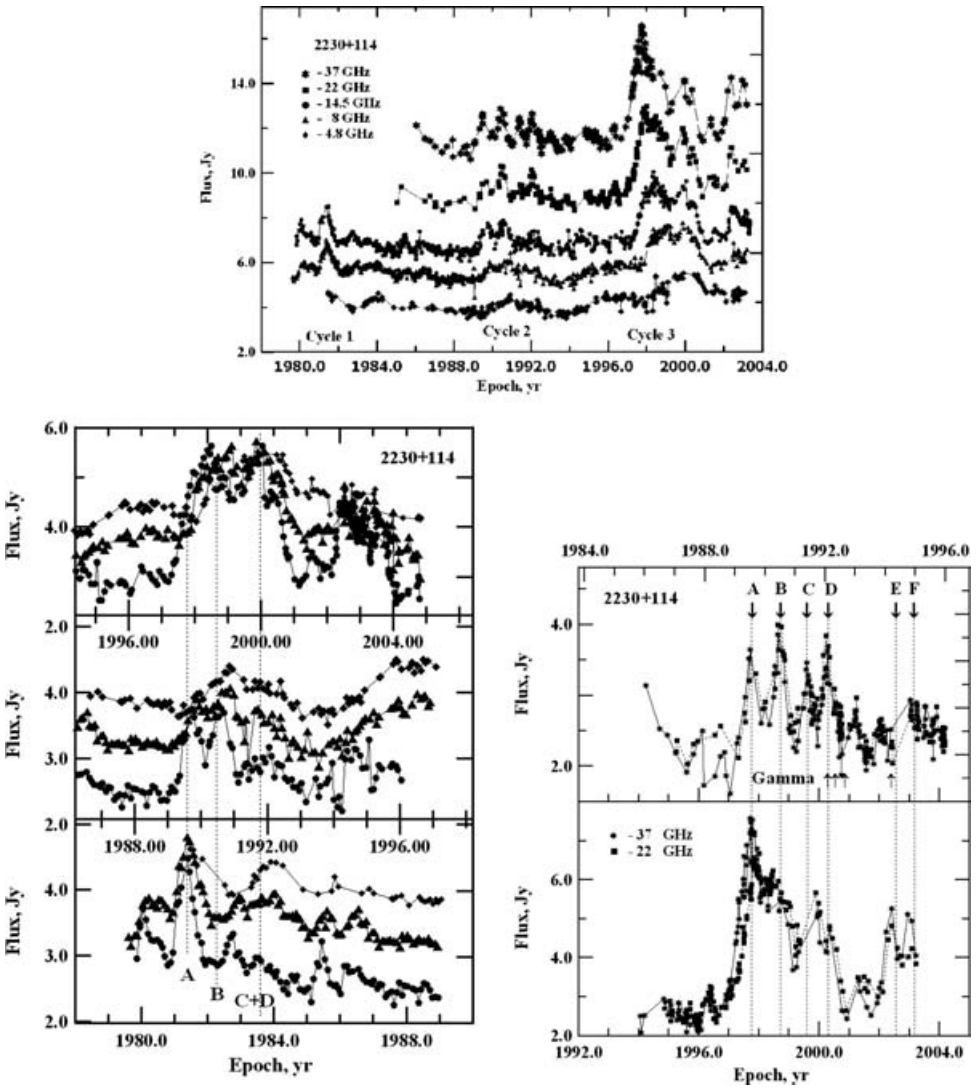


Figure 9. 2230+114. Above: from top to bottom, light curves for 37, 22, 14.5, 8 and 4.8 GHz shifted upwards by 9, 6, 4, 2 and 0 Jy, respectively. Below left-hand side: quasi-periodicity of outbursts at 14.5 GHz (circles), 8 GHz (triangles) and 4.8 GHz (diamonds). Below right-hand side: quasi-periodicity at 37 and 22 GHz. In both the lower figures, the years covered by each individual panel are indicated beneath that panel, with some overlap between panels that cover adjacent time-intervals.

Table 6. Parameters of the time-delay function for core outbursts.

Source	Component	$T_{\max}$ (37 GHz)	α
0458−020	A	1989.1	−1.46
0528+134	D	1995.9	−0.87
0528+134	E	1998.4	−1.22
0528+134	F	1999.8	−1.31
1730−130	A	1996.3	−2.16
2230+114	A2	1989.6	−0.89
2230+114	B2	1990.5	−1.55
2230+114	A3	1997.5	−0.72
2230+114	B3	1997.9	−0.60

VLBI and integrated monitoring data are needed to determine the epoch of the maximum flux and the spectrum of this outburst. The leading 8-GHz maximum of the outburst that took place prior to 1981 should have occurred near 1973.5. However, 8-GHz monitoring data (Dent & Kapitzky 1976) show only slow flux variations with an amplitude of $S \leqslant 1$ Jy during 1970.5–1974.5. If our hypothesis of quasi-periodicity in the activity of the source is correct, then the weak activity observed during the 1970s testifies that the activity as a whole is strongly modulated in amplitude by some geometric effect (e.g. variation of the viewing angle) or some intrinsic reason.

Owing to the merging of suboutbursts C, D and E, F at cm wavelengths, time-lags were determined only for the two main suboutbursts A and B (Table 6, Fig. 9). 2230+114 is the only source for which we were able to analyse outbursts that may belong to different activity cycles. The time-lags for the two periods of activity are correlated with the corresponding outburst amplitudes: suboutbursts A and B of the brightest outburst, with its maximum near 1997.5, show greater time-lags than suboutbursts A and B of the more modest outburst with its maximum near 1989.6 (see below).

Four moderate gamma-ray flares ($S > 7 \times 10^{-7}$ photon cm^{-2} s^{-1}) detected during 1992–1994 coincide with suboutbursts D2 and E2 (Fig. 9, below right-hand panel). Unfortunately, we have no high-resolution VLBI data for epochs prior to 1995. Multi-epoch 43-GHz VLBA observations (Jorstad et al. 2001, 2005) covering the time-interval from 1995 to 2001 reveal three faint ($S \leqslant 0.3$ Jy) superluminal components, which could have been ejected during the final stage of cycle 2 (B1, $T_0 = 1994.12$; B2, $T_0 = 1995.19$; B3, $T_0 = 1996.08$), as well as the two superluminal components B2a and B3a, which seem to be associated with suboutbursts B3 and C3. The variations of the flux densities of the core and new-born jet components are shown in Fig. 11. The frequency-dependent-delay suboutburst A can be classified as a 'core' outburst, and is associated with brightening of the core. Suboutburst B is a mixed outburst, which displays low-frequency delays but is also associated with the appearance of new superluminal components.

7 DISCUSSION

7.1 Types of outbursts

An analysis of the outbursts combined with the detailed structural evolution at 43 GHz shows that only one of the outbursts can be classified as a pure core (2230+114, A) and one as a pure jet (0458−020, C) outburst in terms of both their time-delays and their association with core or jet brightening. Most outbursts are mixed, in the sense that they display both frequency-dependent time-lag s and a connection with the appearance of new jet components. Note that previous classifications of outbursts (Pyatunina et al. 2000; Zhou et al. 2000) were based on low-frequency (5- and 8-GHz) VLBI observations. However, a jet component resolved at 43 GHz would be merged with the core at lower frequencies, so that an outburst classified as a core type at low frequency might be identified as a mixed type at high frequencies. This illustrates the importance of high-frequency VLBI data for probing the early stages of activity within the jet.

It seems likely that the pure core and mixed core-jet outbursts represent fundamentally the same phenomenon: activity in the core that gives rise to the ejection of material along the jet. In this case, the brightness of the ejected material associated with the pure core outburst A in 2230+114 faded before becoming distinct from the observed core at 43 GHz. It is easy to understand the larger number of pure core outbursts at lower frequencies as well: with the lower resolution available, the ejected components are more likely to have faded beyond detection by the time they become distinct from the core. The relatively small number of pure jet outbursts then represent brightening of an optically thin region of the jet well after its ejection from the core, for example, due to the formation of shocks.

7.2 Fine structure of outbursts

Some traces of fine structure can be found in all the outbursts, at least at the highest frequencies. In some of the sources, the fine structure dominates, splitting outbursts into distinct suboutbursts (0528+134, 2230+114), while in others (0458−020 and 1730−130), it degenerates into small fluctuations of the fluxes. Note that the appearance of fine structure in light curves is independent of resolution, but can be hidden due to high optical depth. Savolainen et al. (2002) suggested that outburst fine structure can be induced by shocks that grow and decay in the innermost few tenths of a milliarcsecond. According to theoretical simulations, shocks can be generated by several mechanisms: (i) multiple recollimation shocks, which are induced by the pressure mismatch between the jet and surrounding medium (Gómez et al. 1997), (ii) interactions between helical instability modes that grow due to perturbations to the jet by jet–cloud collisions or precession, with elliptical (Lobanov, Hardee & Eilek 2003) or body waves (Hardee et al. 2001) growing into the jet; and (iii) interactions of the jet with obstacles in its path. The preservation of the positions of individual suboutbursts in outbursts belonging to different activity cycles in 2230+114 may provide important information for distinguishing between these mechanisms. However, it is necessary to carry out similar analyses for more sources, in order to investigate whether this property is common or peculiar to this source.

The presence of fine structure in the outbursts can significantly complicate the identification of a 'starting point' of the activity. Strictly speaking, only information about flux variations at frequencies above ∼40 GHz in combination with 43-GHz VLBI data can address this problem.

7.3 Time-delay as a function of frequency

The parameters of the time-delay function $\Delta T = \Delta T_0 \nu^{\alpha}$ for all events defined for at least four frequencies are given in Table 6. According to theoretical estimates (Gómez, Alberdi & Marcaide 1993; Gómez et al. 1997), the position of the core is expected to depend on the frequency as $r_{\rm core} \propto \nu^{-0.8}$. The frequency-dependent shift of the core position in 3C 345 estimated by Lobanov (1998) turned out to be close to the theorical expectation $r \propto \nu^{(-1.04\pm0.16)}$. If the flow velocity is independent of frequency, then the time-delay is expected

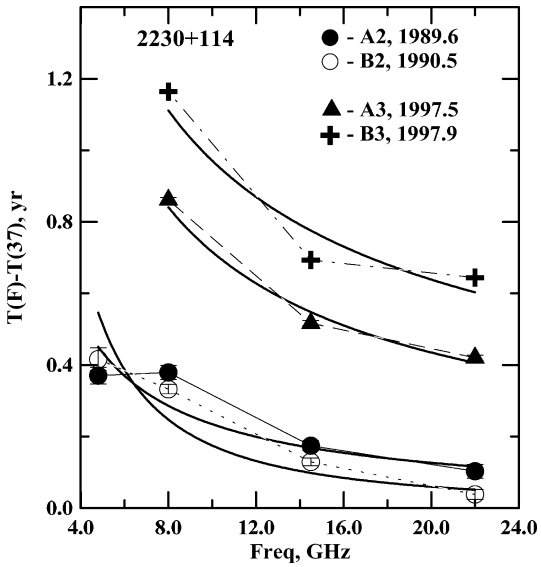


Figure 10. 2230+114. Time-delays as functions of frequency. The bold curves show exponential fits to the observed time-delays.

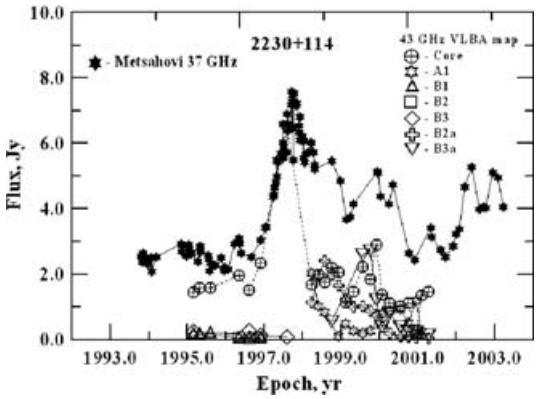


Figure 11. 2230+114. Evolution of the 43-GHz flux densities of the core and jet components (Jorstad et al. 2001, 2005).

to behave similarly. The indices of the time-delay functions given in Table 6 vary from −0.6 (0528+134, B3) to −2.2 (1730−130) with the mean value $\alpha_{\rm mean} = (-1.20 \pm 0.49)$. The time-delay functions for individual events (Figs 3, 6, 8 and 10) show significant dispersions for the time-delays at separate frequencies. If we restrict our consideration to the approximating functions with the smallest residuals (0528+134 – D, E; 2230+114 – A3, B3), the corresponding mean value is $\alpha_{\rm mean} = (-0.85 \pm 0.27)$. Both the 'pessimistic' and 'optimistic' estimates for the mean time-lag index are consistent with the expected value of −0.8, taking into account the fairly large errors. The only exception might be the index for 1730−130.

The shift of the core position between two frequencies is expected to depend on the luminosity of the source (Lobanov 1998):

$$\Delta r \propto L_{\rm syn}^{2/3}.$$

As above, we expect a similar dependence for the time-lags. The relationship between the amplitudes of the outbursts in two subsequent activity cycles in 2230+114 and their time-lags is in qualitative agreement with the expectation (Fig. 10; the outbursts in cycle 3 display both higher amplitudes and larger time-delays). However, the time-lags for individual suboutbursts within a single outburst do not display a similar relation with the suboutburst amplitudes (0528+134). The time-lags for the individual suboutbursts may depend on the dynamical evolution of the underlying perturbation, rather than on their amplitude.

7.4 Outbursts and structural evolution

As was already shown by Savolainen et al. (2002), the emergence of all bright components is correlated with local maximum of the light curves. A comparison of the 37-GHz light curves with the flux densities of the cores and new superluminal components as functions of time (Figs 2, 4, 7, 11) augments the correlation. The flux densities of both the cores and the new-born jet components reach their highest values near the maxima of the 37-GHz light curves, after which they fade.

Some well-studied events (Fig. 12) indicate that the times when the flux densities of new-born components reach their maxima nearly coincide with the times when they experience a sudden increase in their velocity of separation from the core. A similar increase in the velocity of the superluminal component C8* was observed near 1998 in the quasar 3C 279 (Jorstad et al. 2005); note the close coincidence of this epoch with the maximum of the brightest outburst observed in 3C 279 since 1965. This suggests that the flux density may reach its maximum when a shocked region that gives birth to a new jet component becomes optically thin and enters a free-expansion regime, as has been suggested by Gómez et al. (1997) (although changes in brightness occuring simultaneously with accelerations can also result from geometric effects, such as bending of the jet towards or away from the line of sight; see e.g. Homan et al. 2003). Another intriguing phenomenon observed in 2230+114 is the interaction of the stationary component A1 with the moving component B3, when A1 is dragged downstream by B3, and then returns upstream, increasing its flux density (Gómez et al. 2001).

7.5 Conclusions

Our main results can be summarized as follows.

(1) Frequency-dependent time-delays for bright outbursts in four gamma-ray quasars have been estimated and approximated using an exponential function of frequency, $T_{\rm max}(\nu) \propto \nu^{\alpha}$. The time-delays in the sources range from ∼0.3 to ∼1.0 yr. The mean value of the index of the time-delay function is $\alpha_{\rm mean} = (-1.2 \pm 0.5)$, and the maximum value in terms of its magnitude is $\alpha = (-2.2 \pm 0.3)$, for the source 1730−130.

(2) The observed outbursts in 0528+134 and 2230+114 reveal fine structure and consist of narrow (∼1 yr) suboutbursts. Some traces of unresolved fine structure are also seen in 0458−020 and 1730−130. The time-delays and exponential-function indices vary from one suboutburst to another.

(3) Due to the prominent fine structure observed in some outbursts, identification of the starting point of the activity requires information about the spectral evolution at frequencies higher than 40 GHz or the structural evolution at mm wavelengths.

(4) Lower limits for the durations of the activity cycles, or activity time-scales, have been estimated for 0458−020 ($T_{\rm act} \geqslant 16$ yr) and 1730−130 ($T_{\rm act} \geqslant 9$ yr). The results of VLBI imaging at 8 GHz (Britzen et al. 1999b) and 43 GHz (Jorstad et al. 2001, 2005) suggest that the approximate duration of the activity cycle for 0528+134 is $T_{\rm act} \sim 14$ yr. Bright outbursts in 2230+114 repeat with a quasi-period of 8.04 ± 0.30 yr. Although the amplitudes of individual suboutbursts vary from one quasi-period to another, their positions

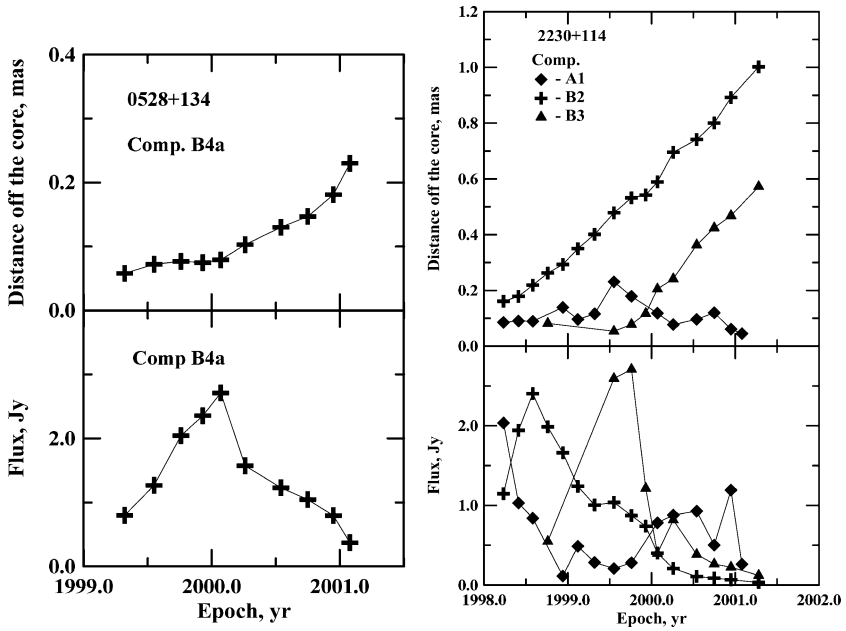


Figure 12. Distance from the core and flux as functions of time for component B4 in **0528+134** (left-hand panel) and the components A1, B2 and B3 in **2230+114** (right-hand panel) (Jorstad et al. 2005).

within the overall outburst are preserved. The time-lags for two adjacent periods of activity in 2230+114 suggest a correlation with outburst amplitude: the brighter outburst shows a greater time-delay. The first maximum of the following bright outburst in 2230+114 is expected to be near 2005.5 ± 0.3.

(5) The maximum flux densities of new jet components often coincide with a sudden increase in their velocities from the core. This suggests that the component's flux reaches its maximum when the shocked region that corresponds to the jet component becomes optically thin and begins to freely expand, as was suggested by Gómez et al. (1997).

ACKNOWLEDGMENTS

The work was supported by the RFBR (grant 05-02-17562). The UMRAO has been supported by a series of grants from the National Science Foundation (NSF) and by funds from the University of Michigan. SGJ was partly supported by the NSF grant (AST 04-06865). This research has made use of the United States Naval Observatory (USNO) Radio Reference Frame Image Database (RRFID). We acknowledge also the MOJAVE and VLBA 2-cm Survey Program teams. Finally, we wish to thank the referee, Matt Lister, for his thorough reading of this manuscript and his helpful and productive comments for improving this paper.

REFERENCES

Agudo ı., Gómez J. L., Gabuzda D. C., Alberdi A., Marscher A. P., Jorstad S. G., 2002, in Ros E., Porcas R. W., Lobanov A. P., Zensus J. A., eds, Proc. 6th European VLBI Network Symposium. BL Lac Phenomenon. Astron. Soc. Pac., San Francisco, p. 115

Aller H. D., Aller M. F., Latimer G. E., Hodge P. E., 1985, ApJS, 59, 513

Aller M. F., Aller H. D., Hughes P. A., Latimer G. E., 1999, ApJ, 512, 601

Bower G. C., Backer D. C., Wright M., Forster J. R., Aller H. D., Aller M. F., 1997, ApJ, 484, 118

Britzen S., Vermeulen R. C., Taylor G. B., Readhead A. C. S., Pearson T. J., Henstock D. R., Wilkinson P. N., 1999a, in Takalo L. O., Sillanpää A., eds, ASP Conf. Ser. Vol. 159, BL Lac Phenomenon. Astron. Soc. Pac., San Francisco, p. 431

Britzen S., Witzel A., Krichbaum T. P., Qian S. J., Campbell R. M., 1999b, A&A, 341, 418

Carswell R. F., Strittmatter P. A., Williams R. D., Kinman T. D., Serkowski K., 1974, ApJ, 190, L101

Dent W. A., Kapitzky J. E., 1976, AJ, 81, 1053

Fey A. L., Boboltz D. A., Charlot P., Fomalont E. B., Lanyi G. E., Zhang L. D., 2005, in Romney J. D., Reid M. J., eds, ASP Conf. Ser. Vol. 340, Future Directions in High Resolution Astronomy: The 10th Anniversary of the VLBA. Astron. Soc. Pac., San Francisco, p. 514

Gómez J. L., 2005, in Romney J. D., Reid M. J., eds, ASP Conf. Ser. Vol. 340, Future Directions in High Resolution Astronomy: The 10th Anniversary of the VLBA. Astron. Soc. Pac., San Francisco, p. 13

Gómez J. L., Alberdi A., Marcaide J. M., 1993, A&A, 274, 55

Gómez J. L., Martí J. M., Marscher A. P., Ibáñez J. M., Alberdi A., 1997, ApJ, 482, L33

Gómez J. L., Marscher A. P., Alberdi A., Jorstad S. G., Agudo I., 2001, ApJ, 561, 161

Hardee P. E., Hughes P. A., Rosen A., Gómez E. A., 2001, ApJ, 555, 744

Hewitt A., Burbidge G., 1993, ApJS, 87, 451

Homan D. C., Lister M. L., Kellermann K. L., Cohen M. H., Ros E., Zensus J. A., Kadler M., Vermeulen R. C., 2003, ApJ, 589, L9

Jorstad S. G., Marscher A. P., Mattox J. R., Aller M. F., Aller H. D., Wehrle A. E., Bloom S. D., 2001, ApJ, 556, 738

Jorstad S. G. et al., 2005, AJ, 130, 1418

Kellermann K. I., Vermeulen R. C., Zensus J. A., Cohen M. H., 1998, AJ, 115, 1295

Kidger M. R., 2000, AJ, 119, 2053

Kranich D., 2003, in Takalo L. O., Valtaoja E., eds, ASP Conf. Ser. Vol. 299, High Energy Blazar Astronomy. Astron. Soc. Pac., San Francisco, p. 3

Krichbaum T. P., Britzen S., Standke K. J., Witzel A., Schalinski C. J., Zensus J. A., 1995, Proc. Nat. Acad. Sci. USA, 92, 11377

Krichbaum T. P., Witzel A., Graham D., Lobanov A. P., 1997, in Barvanis R., Phillips R. B., eds, Millimeter-VLBI Science Workshop. MIT Press, Massachusetts, p. 3

Lehto H. J., Valtonen M. J., 1996, ApJ, 460, 207

Lister M. L., 2001, ApJ, 561, 676

Lister M., Homan D., 2005, AJ, 130, 1389

Lobanov A. P., 1998, A&A, 330, 79

Lobanov A. P., Roland J., 2002, in Ros E., Porcas R. W., Lobanov A. P., Zensus J. A., eds, Proc. 6th European VLBI Network Symposium. Max-Planck-Institut für Radioastronomie, Bonn, p. 121
Lobanov A. P., Krichbaum T. P., Graham D. A., 2000, A&A, 364, 391
Lobanov A. P., Hardee P. E., Eilek J., 2003, New Astron. Res., 47, 629
Marscher A. P., 1996, in Miller H. R., Webb J. R., Noble J. C., eds, ASP Conf. Ser. Vol. 110, Blazar Variability. Astron. Soc. Pac., San Francisco, p. 248
Marscher A. P., 2001, in Peterson B. M., Polidan R. S., Pogg R. W., eds, ASP Conf. Ser. Vol. 224, Probing the Physics of Active Galactic Nuclei by Multiwavelengths Monitoring. Astron. Soc. Pac., San Francisco, p. 23
Marscher A. P., Jorstad S. G., Mattox J. R., Wehrle A. E., 2002, ApJ, 577, 85
Mukherjee R. et al., 1997, ApJ, 490, 116
Mukherjee R. et al., 1999, ApJ, 527, 132
Pian E., 2003, in Takalo L. O., Valtaoja E., eds, ASP Conf. Ser. Vol. 299, High Energy Blazar Astronomy. Astron. Soc. Pac., San Francisco, p. 37
Pohl M. et al., 1995, A&A, 303, 383
Pursimo T. et al., 2000, A&AS, 146, 141
Pyatunina T. B., Marchenko S. G., Marscher A. P., Aller M. F., Aller H. D., Teräsranta H., Valtaoja E., 2000, A&A, 358, 451
Pyatunina T. B., Rachimov I. A., Zborovskii A. A., Gabuzda D. C., Jorstad S. G., Teräsranta H., Aller M. F., Aller H. D., 2003, in Takalo L. O., Valtaoja E., eds, ASP Conf. Ser. Vol. 299, High Energy Blazar Astronomy. Astron. Soc. Pac., San Francisco, p. 89
Pyatunina T. B., Kudravtseva N. A., Gabuzda D. C., Jorstad S. G., Aller M. F., Aller H. D., Teräsranta H., 2005, in Romney J. D., Reid M. J., eds, ASP Conf. Ser. Vol. 340, Future Directions in High Resolution Astronomy: The 10th Anniversary of the VLBA. Astron. Soc. Pac., San Francisco, p. 13
Raiteri C. M. et al., 2001, A&A, 377, 396
Reuter H.-P. et al., 1997, A&AS, 122, 271
Savolainen T., Wiik K., Valtaoja E., Jorstad S. G., Marscher A. P., 2002, A&A, 394, 851
Sillanpää A., 1999, in Chakrabarti, ed., Observational Evidence for Black Holes in the Universe. Kluwer, Dordrecht, p. 209
Steppe H., Salter C. J., Chini R., Kreysa E., Brunswig W., Lobato Pérez J., 1988, A&AS, 75, 317
Steppe H., Liechti S., Mauersberger R., Kömpe C., Brunswig W., Ruiz-Moreno M., 1992, A&AS, 96, 441
Steppe H. et al., 1993, A&AS, 102, 611
Sundelius B., Wahde M., Lehto H. J., Valfonen M. J., 1997, ApJ, 484, 180
Teräsranta H. et al., 1998, A&AS, 132, 305
Teräsranta H., Wiren S., Koivisto P., 2003, in Takalo L. O., Valtaoja E., eds, ASP Conf. Ser. Vol. 299, High Energy Blazar Astronomy. Astron. Soc. Pac., San Francisco, p. 235
Teräsranta H. et al., 2004, A&A, 427, 769
Teräsranta H., Wiren S., Koivisto P., Saarinen V., Hovatta T., 2005, A&A, 440, 409
Valtaoja E., Lähteenmäki A., Teräsranta H., Lainela M., 1999, ApJS, 120, 95
Valtaoja E., Teräsranta H., Tornikoski M., Sillanpää A., Aller M. F., Aller H. D., Hughes P. A., 2000, ApJ, 531, 744
Wright A. E., 1984, Proc. Austr. Astron. Soc., 5, 510
Zhang Y. F., Marscher A. P., Aller H. D., Aller M. F., Teräsranta H., Valtaoja E., 1994, ApJ, 432, 91
Zhou J. F., Hong X. Y., Jiang D. R., Venturi T., 2000, ApJ, 540, L13

This paper has been typeset from a TEX/LATEX file prepared by the author.